IEEE Access
Multidisciplinary | Rapid Review | Open Access Journal

Received July 19, 2020, accepted July 26, 2020, date of publication August 4, 2020, date of current version August 17, 2020.

*Digital Object Identifier 10.1109/ACCESS.2020.3014123*

# Using Polarization-Diverse Wave-Coefficients for Aerospace Target Recognition

**XIAOMIN JIANG, YINGXIN LAI, (Member, IEEE), SHANJIN WANG, AND YUE SONG**
School of Electronic Engineering and Intelligentization, Dongguan University of Technology, Dongguan 523000, China

Corresponding author: Xiaomin Jiang (efforsn@163.com)

This work was supported by the National Natural Science Foundation of China under Grant 61701116.

**ABSTRACT** Wave-coefficients (WCs) based target recognition can be theoretically applied to any a frequency range, with increased sensitivity to aspect angle at higher frequencies. When it is utilized to a frequency range in resonance region, the WCs can tolerate fairly big aspect variation and contain enough target information, bringing a competitive advantage in multitudinous target features. Four polarization channel WCs are introduced and independently utilized to identify four aerospace targets under noise and noise-free circumstances. To take full advantage of the WCs in different polarization channels, a novel radar aerospace target recognition method based on multi-polarization channel WCs is proposed in this article. The majority vote rule and a maximum discrepancy rule are combined to identify a target when four polarization channel WCs are available at the same time. Simulation results on four aircraft models show that the proposed technique achieves a recognition performance at least comparable to the best single channel performance.

**INDEX TERMS** Pattern recognition, radar target recognition, radar target classification, wave-coefficient.

## I. INTRODUCTION

Real-world empirical target recognition using some target feature is one of the most challenging section in radar technology. Substantial research work has been conducted on this topic. Selection of a proper target feature is of essential importance to a successful target recognition [1], and a variety of target features are exploited for target identification. The high resolution range profile (HRRP) represents the distribution of the scattering centers along the radar line-of-sight (LOS). HRRP based radar automatic target recognition (RATR) is intensively studied and numerous relevant literatures have been reported openly [2]–[6]. Poles based RATR has drawn considerable attention due to its tremendous advantage that it is irrelevant to the target azimuth [7]–[11]. The synthetic aperture radar (SAR) image offers an intuitionistic contour profile of the target, besides, it has the advantages of penetration ability through obstacles and day-night operation. Thus, it makes SAR image a well-known radar target feature [12]–[15]. There is a general consensus among the researchers that no single feature vector is optimal on all occasions. Developing new target features is still a significant research aspect in RATR community. Micro-doppler signatures were utilized to discriminate moving target in [16]–[19]. The polarization scattering characteristics of chaff clouds were studied and a support vector machine (SVM) classification method was presented in [20]. In [21], the authors proposed a linear polarisation images based method for target recognition in passive millimeter-wave imaging system.

Two-dimensional (2D) target identification with a feature vector termed wave-coefficients (WCs), was proposed in [22]. WC concept was extended to three-dimensional (3D) targets in [23], where four aerospace targets were considered. Experimental results show that the WCs are with increased sensitivity to aspect angle at higher frequencies. Theoretically, the WCs's sensitivity to aspect angle can be effectively relaxed by reducing the operating frequency of the radar. However, if the operating frequency is chosen too low, the targets are equivalent to a scattering point, and WCs based target recognition will lose effectiveness. An operating frequency range in resonance region was proposed in [23], in which the WCs can tolerate big aspect variation, bringing a decided advantage in a large number of target features. Because there are few target features for aerospace target which are able to provide reliable target recognition in resonance region. Besides, the WCs method has merits such as flexible application, easy acquisition, etc. However, literature [23] only took

The associate editor coordinating the review of this manuscript and approving it for publication was Jinming Wen.

one single polarization channel WCs into account. At some aspect angles, the WCs are not able to provide enough distinction, resulting in a comparatively poor recognition performance. It needs to be pointed out that echoes from different polarization channels (for instance, in this article, horizontal-$\phi$ component H-H, horizontal-$\theta$ component H-V, vertical-$\phi$ component V-H, vertical-$\theta$ component V-V) contain or enhance certain target information [24]. Echoes from different polarization channels can be obtained simultaneously by polarimetric radars. A comparison among the recognition performances with different polarization channels is an important work. Besides, if WCs extracted from different polarization channels are fused to recognize a target, it is expected that the recognition performance can be improved or guaranteed. Motivated by this purpose, we propose a multi-polarization channel WCs algorithm to raise the identification rate and enhance the robustness of the WCs scheme in this article.

The rest of the article is organized as follows. Section II introduces the WCs of a 3D target. Section III elaborates the recognition procedures of the proposed algorithm. A discussion of the characteristics of the WCs and the detailed recognition performance in noise and noise-free environment are provided in Section IV. Section V comes the conclusions.

## II. CONCEPT OF THE WCS OF A 3D TARGET

The scattered far fields of an unknown target are expressed by the superposition of the spherical waves, and the superposition coefficients are termed WCs. Suppose a plane wave is illuminating on a conducting target with arbitrary shape along the z-axis, and the electric field is polarized in x-axis. The scattered field far away can be written in the form as follows:

$$E_\theta^s(\theta,\phi,k) = \frac{jE_0\cos\phi_0}{k}\sum_{n=1}^{\infty}\frac{(2n+1)}{n(n+1)}\left\{P_n(\theta,\phi)a_n(k)P_n^{(1)}(\cos\theta_0) + Q_n(\theta,\phi)b_n(k)\left[\cos\theta_0 P_n^{(1)}(\cos\theta_0) - \tau_n P_n^2(\cos\theta_0)\right]\right\} \tag{1}$$

$$E_\phi^s(\theta,\phi,k) = \frac{jE_0\sin\phi_1}{k}\sum_{n=1}^{\infty}\frac{(2n+1)}{n(n+1)}\left\{M_n(\theta,\phi)b_n(k)P_n^{(1)}(\cos\theta_1) + L_n(\theta,\phi)a_n(k)\left[\cos\theta_1 P_n^{(1)}(\cos\theta_1) - \tau_n P_n^2(\cos\theta_1)\right]\right\} \tag{2}$$

where $E_\theta^s$ and $E_\phi^s$ denote $\theta$ and $\phi$ component of the scattered field respectively. n is the subscript of the summation. Coefficients $P_n$, $Q_n$, $L_n$ and $M_n$ are the WCs. $k=\omega/c$ is the wave number, and $\tau_n = \begin{cases} 0 & n=1 \\ 1 & n=others \end{cases} \cdot P_n^m(\cos\theta)$ denotes the associated Legendre Polynomial, and $P_n^{(1)}(\cos\theta) = \partial P_n^1(\cos\theta)/\partial(\cos\theta)$. $a_n$ and $b_n$ are defined as

$$a_n(k)=\hat{J}_n(ka_e)/\hat{H}_n^{(2)}(ka_e),\quad b_n(k)=\hat{J}_n'(ka_e)/\hat{H}_n^{(2)\prime}(ka_e) \tag{3}$$

where $\hat{J}_n(\chi)$ and $\hat{H}_n^{(2)}(\chi)$ are the Ricatti-Bessel and Ricatti-Hankel functions expressed as $\hat{J}_n(\chi) = \chi j_n(\chi)$ and $\hat{H}_n^{(2)}(\chi) = \chi h_n^{(2)}(\chi)$ with $j_n(\chi)$ and $h_n^{(2)}(\chi)$ the spherical Bessel and Hankel functions, respectively. $a_e$ is the effective radius defined by $a_e = d/2$ with $d$ the minimum diameter of the sphere which enclose the target in this work.

There are many ways to obtain the WCs [25]–[27]. A method termed "Galerkin match" [28] is applied to extract the WCs. Take $\theta$ component for example, match (1) by using $a_m^*(k)$ and $b_m^*(k)$ as the "weighting" function respectively, where "$*$" represents the complex conjugate, then integrate over the operating frequency band, we have:

$$\sum_{n=1}^{2N} Z_{mn}^1 B_n = g_m^1,\quad m=1,2,\cdots M,\quad M\geq N \tag{4}$$

$$\sum_{n=1}^{2N} Z_{mn}^2 B_n = g_m^2 \tag{5}$$

where $B_n$ are the cascade of $P_n$ and $Q_n$, N is the truncation term of $P_n$ and $Q_n$, and M is the truncation term of $a_m^*(k)$. $Z_{mn}^1$ and $g_m^1$ can be expressed as follows:

$$Z_{mn}^1 = \begin{cases} jE_0\cos\phi_0 P_n^{(1)}(\cos\theta_0)\int_{k_{\min}}^{k_{\max}} a_n(k)*a_m^*(k)/k\,\mathrm{dk} \\ \qquad 1\leq \mathrm{n}\leq \mathrm{N} \\ jE_0\cos\phi_0\cos\theta_0 P_1^{(1)}(\cos\theta_0)\int_{k_{\min}}^{k_{\max}} b_1(k)*a_m^*(k)/\mathrm{kdk} \\ \qquad \mathrm{n}=\mathrm{N}+1 \\ jE_0\cos\phi_0\left[\cos\theta_0 P_{n-N}^{(1)}(\cos\theta_0) - P_{n-N}^2(\cos\theta_0)\right]* \\ \int_{k_{\min}}^{k_{\max}} b_{n-N}(k)*a_m^*(k)/k\,\mathrm{dk}\quad \mathrm{N}+2\leq \mathrm{n}\leq 2*\mathrm{N} \end{cases} \tag{6}$$

$$g_m^1 = \int_{k_{\min}}^{k_{\max}} a_m^*(k)\cdot E_\theta^s(\theta,\phi,k)dk \tag{7}$$

$Z_{mn}^2$ and $g_m^2$ share the same form as $Z_{mn}^1$ and $g_m^1$ respectively just by replacing $a_m^*(k)$ with $b_m^*(k)$. Combine (4) and (5), we obtain the following linear equations:

$$\sum_{n=1}^{2N} Z_{ln}B_n = g_l,\quad l=1,2,\cdots 2M \tag{8}$$

$Z_{ln}$ and $g_l$ are given as follows:

$$Z_{ln} = \begin{bmatrix} Z_{mn}^1 \\ Z_{mn}^2 \end{bmatrix},\quad g_l = \begin{bmatrix} g_m^1 \\ g_m^2 \end{bmatrix} \tag{9}$$

Similarly, when $\phi$ component is taken into account, use the same procedure as $\theta$ component, linear equations of the same form as (8) are obtained and corresponding $Z_{mn}^1$ and $g_m^1$ can

be given as follows:

$$Z^1_{mn} = \begin{cases} jE_0 \sin\phi_1 \cos\theta_1 P_1^{(1)}(\cos\theta_1) \\ \int_{k_{\min}}^{k_{\max}} a_1(k) * a_m^*(k)/\mathrm{kdk\ n} = 1 \\ jE_0 \sin\phi_1 \left[\cos\theta_1 P_n^{(1)}(\cos\theta_1) - P_n^2(\cos\theta_1)\right] * \\ \int_{k_{\min}}^{k_{\max}} a_n(k) * a_m^*(k)/k\mathrm{dk}\ 2 \le \mathrm{n} \le \mathrm{N} \\ jE_0 \sin\phi_1 P_{n-N}^{(1)}(\cos\theta_1) \int_{k_{\min}}^{k_{\max}} b_{n-N}(k) * a_m^*(k)/k\mathrm{dk} \\ \mathrm{N}+1 \le \mathrm{n} \le 2*\mathrm{N} \end{cases} \tag{10}$$

$$g_m^1 = \int_{k_{\min}}^{k_{\max}} a_m^*(k) \cdot E_\phi^s(\theta, \phi, k) dk \tag{11}$$

$Z^2_{mn}$ and $g^2_m$ have the same form as $Z^1_{mn}$ and $g^1_m$ respectively by replacing $a^*_m(k)$ with $b^*_m(k)$.

The scattered far fields are obtained by simulation software FEKO and the WCs are acquired through solving (8) by the method of conjugate gradient (CG) under the least-square (LS) constraint. The back-scattering scenario is considered in this work. Thus the H-V and the V-H yield the same results, and only three polarization channels are investigated.

## III. IMPLEMENTATION OF MULTI-POLARIZATION WCS FOR AEROSPACE TARGET RECOGNITION

The right hand of (8) changes with the incident angles, however, the same basis functions are utilized to expand the scattered fields. Therefore, matrix Z in (8) is irrelevant to the aspect angle. The targets' sensitivity to azimuth angle is totally embodied in the WCs. Simulation results in [22], [23] show that the WCs' sensitivity to azimuth angle is directly proportional to the working frequency. Due to the properties of $\hat{J}_n(\chi)$ and $\hat{H}_n^{(2)}(\chi)$, the dimension of the WCs is augmented with increasing of the operating frequency. An ideal target feature should contain ample information of the target and keep low sensitivity to the aspect angle. Thus, the operating frequency should be appropriately chosen to strike a balance between target information and sensitivity to the azimuth angle. A frequency band in resonance region is proposed in [23], in which the WCs are able to tolerate big aspect variation and contain enough target information at the same time. To take full advantage of different polarization channel WCs, a multiple polarization WCs method is proposed in this work to recognize aerospace targets. The correlation coefficient (CC) is applied to evaluate the similarity between two WCs.

Let $B(i,j) = \{B_n(i,j) : n = 0, 1, \cdots, N\}$ denote the $j$-th WC stored in the feature database for target $i$, and $X = \{X_n : n = 0, 1, \cdots, N\}$ denote a WC extracted from the received radar echoes from a candidate target. The CC is defined as follows:

$$C(i,j;X) = \frac{\left|\sum_{n=0}^{N} B_n(i,j) \cdot X_n^*\right|}{\sqrt{\sum_{n=0}^{N} |B_n(i,j)|^2 \cdot \sum_{n=0}^{N} |X_n|^2}} \tag{12}$$

Clearly, $0 \le C \le 1$ and $C = 1$ if and only if the two WCs are in proportion.

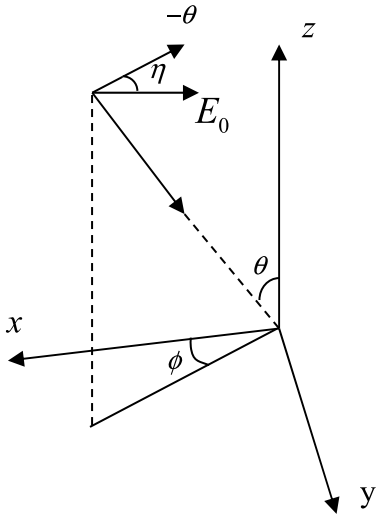


**FIGURE 1.** Coordinate system used in this work.

In view of the above-mentioned properties and the decision rule, multiple polarization WCs based aerospace target recognition is performed following the procedure below:

(1) Study the WCs' sensitivity to the aspect angle, and determine the sampling interval angle along $\theta$ direction and $\phi$ direction. Store the WCs of the candidate targets within the aspect range of interest as the database. Use $B_i(\theta, \phi)$ to denote the WC for target i at the azimuth $(\theta, \phi)$.

(2) Extract the WCs from the received radar echoes. Estimate the target aspect $(\theta_0, \phi_0)$ with respect to the radar.

(3) Assume that the estimate errors in $\theta$ direction and $\phi$ direction are within $\pm\Delta\theta$ and $\pm\Delta\phi$, respectively. Find all WCs in the azimuth angle scope, i.e. $\theta_o - \Delta\theta \le \theta \le \theta_o + \Delta\theta$, $\phi_o - \Delta\phi \le \phi \le \phi_o + \Delta\phi$, and calculate the CCs.

(4) Exploit each single polarization channel WCs to identify an unknown target independently.

Set a threshold CC, then identify the undecided target to be the one in the candidate targets that provides the maximum CC which is greater than the threshold CC at the same time. Then use the majority vote rule to determine the unknown target, that is, we identify the unknown target as the one voted by the most polarization channels. Correspondingly, the target is undetermined if there is at least another one target which has the same poll.

For the undetermined target, the maximum discrepancy rule is applied to determine the class. The discrepancy is defined as the difference between the largest CC and the second largest CC among all targets. Use the polarization

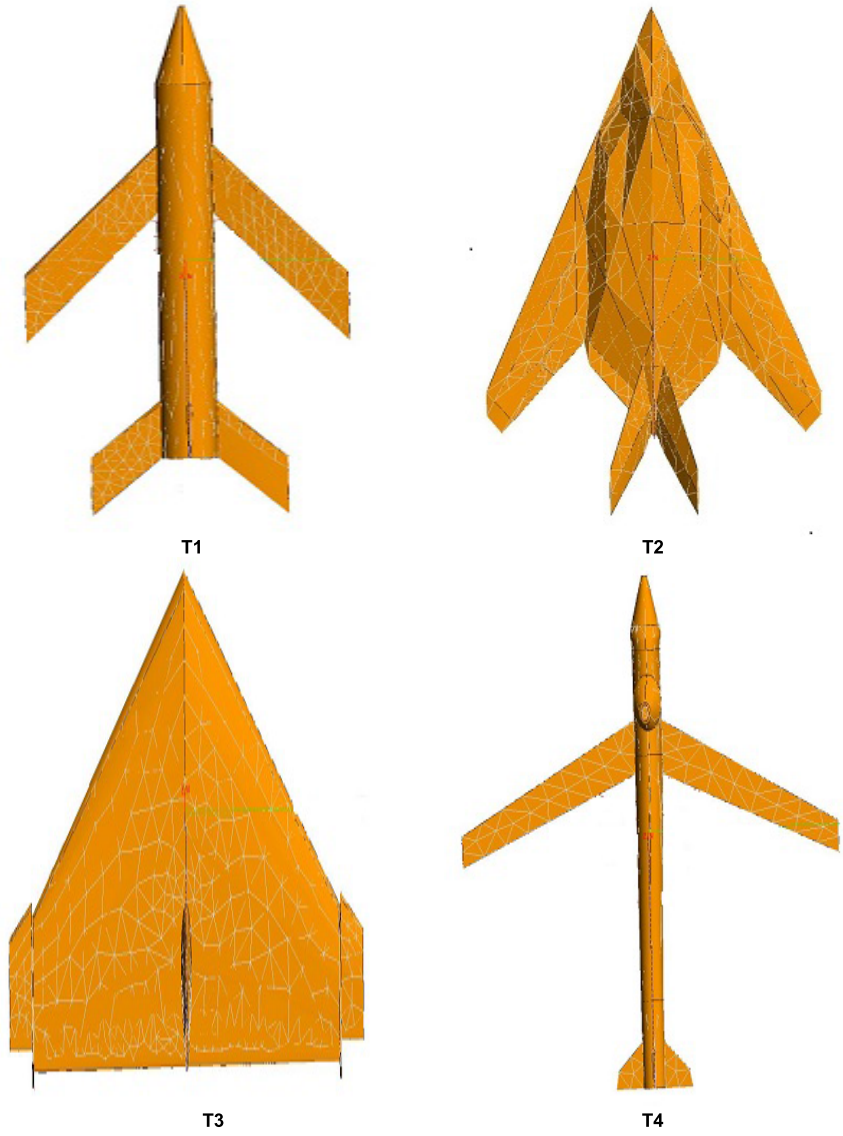


**FIGURE 2.** Four scaled aircraft target models.

channel WCs that provide the maximum discrepancy at the aspect range of interest to identify the target.

## IV. NUMERICAL RESULTS

The coordinate system used in the simulation is shown in Figure 1. $\theta$ represents the angle between the incident direction and -z axis, $\phi$ denotes the angle between the projection of the incident wave on xy coordinate plane and -x axis and $\eta$ is the angle between $-\theta$ direction and the orientation of the incident electric field. In this article, four scaled imitative aircraft models as shown in Figure 2 are chosen as the candidate targets. For the convenience of description, we use T1, T2, T3 and T4 to notate the four candidate targets in the rest of this article. The sizes of them are illustrated in Table 1. Zero degree azimuth is defined as the nose-on direction, and 90 degree is in the wing direction. The centers of the planes and the origin coincide. The simulation frequency band is set to be 300 MHz-600 MHz in this study.

**TABLE 1.** The dimensions of the four targets.

| Targets | Length(m) | Width (m) | Height (m) |
|---|---|---|---|
| T1 | 2.0 | 1.0 | 0.405 |
| *T2* | 2.0 | 1.3 | 0.210 |
| T3 | 1.3 | 2.0 | 0.394 |
| *T4* | 2.0 | 1.9 | 0.274 |

### A. DISTINCTION OF THE WCS

The truncation term in (8) is set to be 20 according to the simulation frequency and the length of the targets. Four single channel WCs with randomly selected incident aspect are

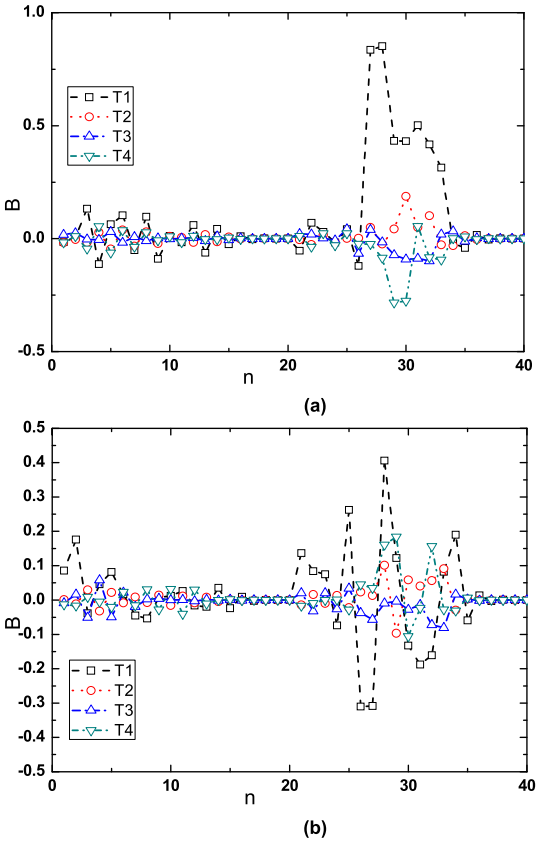


**FIGURE 3.** The $\theta$ component WCs of the four candidate targets with $\theta_i = 174^\circ$, $\phi_i = 59^\circ$, $\eta = 0°$: (a) real part and (b) imaginary part.

shown in Figure 3. As expected, the WCs are different from each other, which indicates that they are a potential feature vector that may be exploited for target recognition.

### *B. THE WCS' SENSITIVITY TO ASPECT ANGLE*

The WCs' sensitivity to aspect angle determines the applicability of the WCs based radar target recognition technique. If the sample intervals of the aspects in both azimuth and elevation directions are too small, too many WCs need to be stored in the data base. The CCs with adjacent aspects are studied to offer guidance on choosing the aspect sample intervals. The aspect matching width (AMW) is introduced to evaluate the WCs' sensitivity to the aspect angle. Assume that $\sigma$ is a prescribed CC threshold, AMW is defined as $AMW = \alpha_1 - \alpha_2$, where $\alpha_1$ and $\alpha_2$ are the minimum and maximum aspect values, respectively, which satisfy the following limitation

$$CC(T_m, \alpha_n, \alpha_0) \geq \sigma, \quad m = 1, 2, 3, 4 \;\; n = 1, 2 \qquad (13)$$

Here, $\alpha_0$ is called the middle angle. AMWs for each target in three polarization channels are studied, and typical AMWs of the candidate targets at two middle angles $\phi = 69°$ and $\phi = 81°$ are plotted in Figure 4. It can be observed that the AMW varies from target to target. For a given target, AMW changes with the middle angles and polarization channels. Provided that $\sigma$ is set to be 0.95, thebiggest AMW

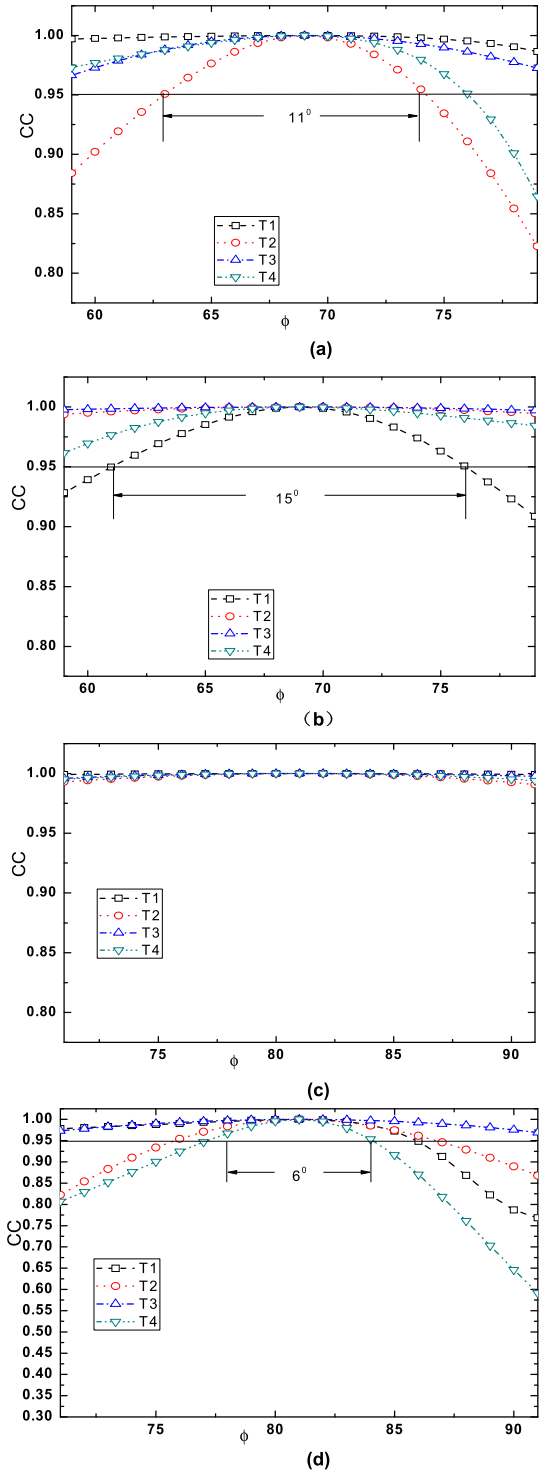


**FIGURE 4.** AMWs of the four candidate targets for $\theta_i = 174^\circ$: (a) middle angle $\phi = 69°$, VH polarization, (b) middle angle $\phi = 69°$, VV polarization, (c) middle angle $\phi = 81°$, HH polarization, (d) middle angle $\phi = 81°$, HV polarization.

in Figure 4 is even bigger than the aspect search window which is 20 degrees in this article. The smallest AMW shown in Figure 4 belongs to target T2 at $\phi = 81°$ in HV polarization channel, however, which still attains 6 degrees. When constructing the WC database, if we study the AMWs in all aspects range of interest (because of structural symmetry,

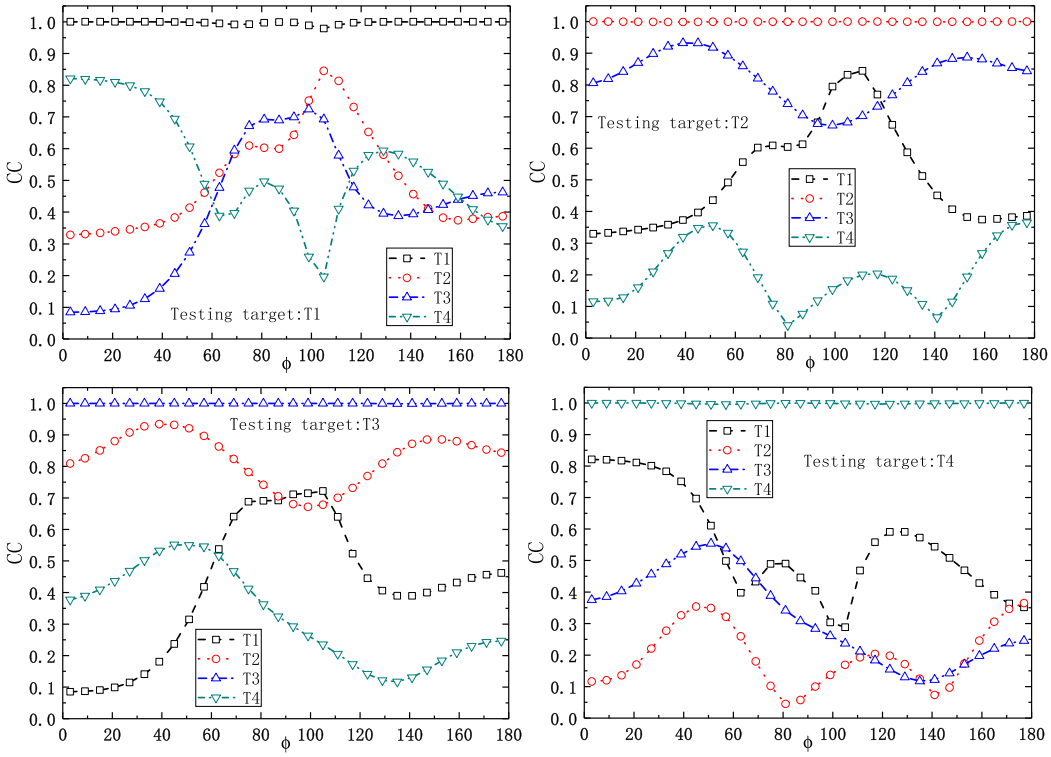


**FIGURE 5.** The CCs between the testing target and the four known targets at all the testing azimuths angles in VV channel.

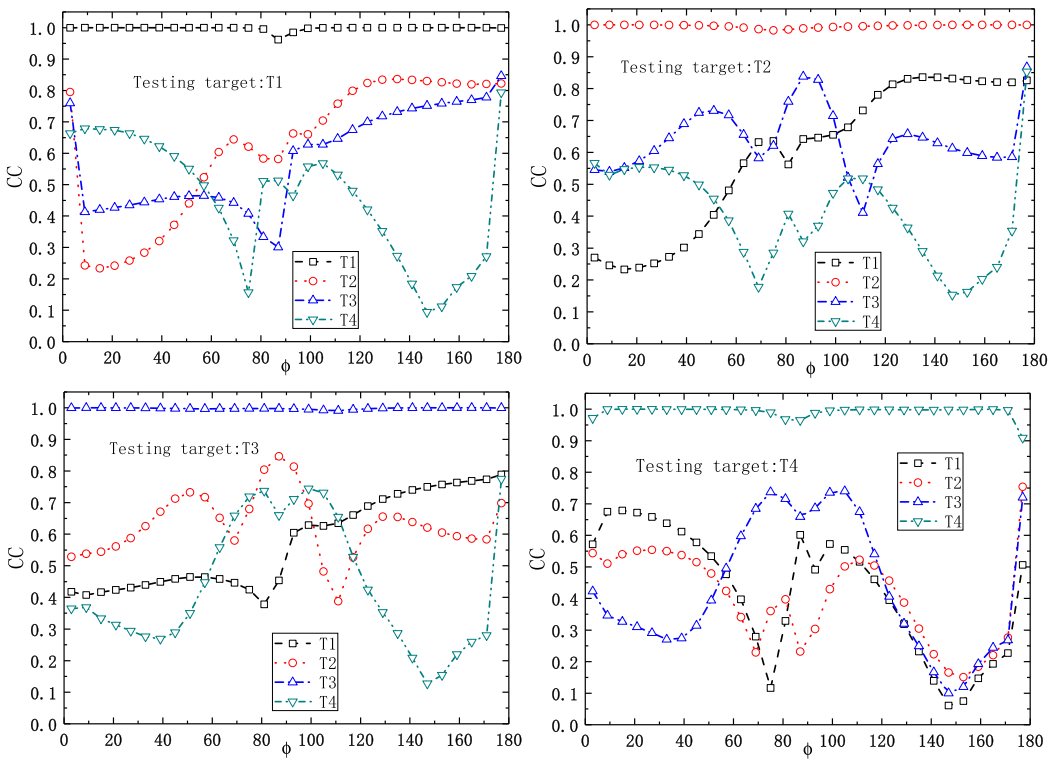


**FIGURE 6.** The CCs between the testing target and the four known targets at all the testing azimuths angles in VH channel.

aspect range of interest along $\theta$ direction and $\phi$ direction are 0°-360° and 0°-180°, respectively), the sampling interval should vary with the the middle angle, thus the number of WC stored in the template database can be greatly reduced.

### C. WC BASED TARGET RECOGNITION IN NOISE-FREE ENVIRONMENT

As the AMWs for all the targets are large enough, there is little burden to store the WCs within the aspect range of interest. For each target, the recognition performance in all three polarization channels are considered. In each channel, the WCs of the candidate targets are uniformly stored with an increment of 6 degrees along $\phi$ direction and $\theta$ is fixed to $174^{\circ}$. Therefore, 31WCs are stored for each object with $\phi = 0°,\ 6°,\ 12° \cdots 180°$. The azimuth angles for testing are uniformly sampled and they are $\phi = 3°,\ 9°,\ 15° \cdots 177°$. For saving the space of this article, the CCs between the testing target and the candidate targets in VV and VH channel are shown in Figure 5 and Figure 6 respectively. In each channel, target T1, T2, T3 and T4 are in turn taken as the testing target.

All figures show that the CCs between the testing target and the matched target are the biggest at all 30 azimuth angles under examination, which indicates that the recognition rate is 100% under the noise-free scenario. However, the target distinction exists significant difference between different polarization channels. For example, in VV channel, there are only nice distinctions between target T2 and T3 at some testing azimuth angles, but there are much wider disparities in WCs between the two targets in VH channel, as the CCs between the two targets are fairly small. The same situation happens among the other targets. This experimental result reflects that WCs in different polarization channels embody different structural information of the target, which urges us to recognize a target by utilizing multiple polarization channel WCs.

### D. WC BASED TARGET RECOGNITION IN GAUSSIAN NOISE CONTAMINATED ENVIRONMENT

In order to evaluate the recognition performance of the proposed method under noise contaminated environment, we add simulated Gaussian white noise to the received echoes. The signal-to-noise (SNR) is defined as

$$SNR = 10 \log_{10} \frac{P_0}{\rho^2} \tag{14}$$

where $P_0$ denotes the power of the received sequence, and $\rho^2$ represents the noise power. The WC at two randomly chosen aspect angles $\phi = 70°$ and $\phi = 95°$ are investigated to compare the performances of our proposed method to each single polarization channel performance. Five hundred simulations are conducted at each SNR level and the threshold CC is set to be 0.9. Several representative correctly recognized ratios versus SNR are plotted in Figure 7.

The experimental results show that the recognition performances in different polarization channels of a given target differs significantly. For example, the recognition rate of target T1 at $\phi = 70°$ in HH channel under SNR = 0dB is even greater than that obtained in VV channel under SNR = 15dB. Meanwhile, different recognition performances are achieved for different targets in a prescribed polarization channel.

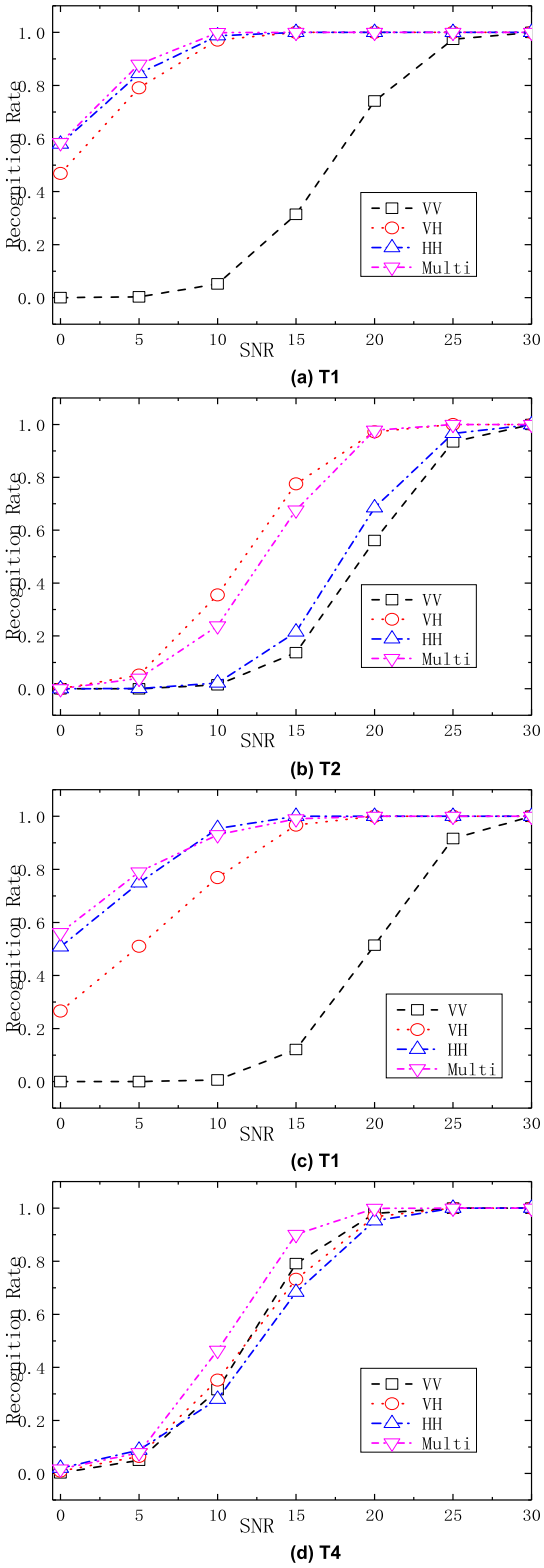


**FIGURE 7.** The correct recognition ratio with respect to SNR at two randomly selected aspect angles: (a) for T1, $\phi = 70°$, (b) for T2, $\phi = 70°$, (c) for T1, $\phi = 95°$, (d) for T4, $\phi = 95°$.

Besides, the recognition performance is closely relevant to the aspect angles. Therefore, it is hard to tell which single channel is superior to the other channels. From the results

given we find that if two polarization channels give a similar performance that is better than that of the third channel, the proposed scheme will yield a recognition performance which is superior to all single channel results. The conclusion holds the same when three channels produce a similar recognition performance. The worst case happens when two channels provide a similar result that is poorer than that of the third channel, in which the proposed scheme will yield a identification performance that is slightly inferior to the third channel. However, the general circumstance is there is not a prior information to tell which polarization channel gives a more reliable recognition result. While the proposed scheme is able to guarantee a performance that is superior to all single channel performances or at least comparable to the best single channel result.

## V. CONCLUSION

Four polarization channel WCs are introduced and exploited for aerospace target recognition in this article. The WCs of a specified target show distinct differences in different channels, which implies that WCs from different channels contain different structural information. Every single channel WCs can be utilized to identify a radar aerospace target independently. It is difficult to tell which polarization channel is superior to the other ones. To sufficiently take advantage of the comprehensive target information, a multi-polarization WCs method that combines the majority vote rule and the maximum discrepancy rule is proposed to improve the identification performance. Simulation results on four aircraft models reveal that the proposed method guarantee a performance that is superior to all single channel results or slightly inferior to the best single channel recognition performance.

## REFERENCES

[1] H.-J. Li and S.-H. Yang, "Using range profiles as feature vectors to identify aerospace objects," *IEEE Trans. Antennas Propag.*, vol. 41, no. 3, pp. 261–268, Mar. 1993.
[2] K. Liao, J. Si, F. Zhu, and X. He, "Radar HRRP target recognition based on concatenated deep neural networks," *IEEE Access*, vol. 6, pp. 29211–29218, 2018.
[3] C. Guo, Y. He, H. Wang, T. Jian, and S. Sun, "Radar HRRP target recognition based on deep one-dimensional residual-inception network," *IEEE Access*, vol. 7, pp. 9191–9204, 2019.
[4] L. Du, P. Wang, H. Liu, M. Pan, F. Chen, and Z. Bao, "Bayesian spatiotemporal multitask learning for radar HRRP target recognition," *IEEE Trans. Signal Process.*, vol. 59, no. 7, pp. 3182–3196, Jul. 2011.
[5] D. Zhou, "Radar target HRRP recognition based on reconstructive and discriminative dictionary learning," *Signal Process.*, vol. 126, pp. 52–64, Sep. 2016.
[6] C. Zhao, X. He, J. Liang, T. Wang, and C. Huang, "Radar HRRP target recognition via semi-supervised multi-task deep network," *IEEE Access*, vol. 7, pp. 114788–114794, 2019.
[7] D. Blanco, D. P. Ruiz, E. Alameda-Hernandez, and M. C. Carrion, "Extinction pulses synthesis for radar target discrimination using $\beta$-splines, new E-pulse condition," *IEEE Trans. Antennas Propag.*, vol. 54, no. 5, pp. 1577–1585, May 2006.
[8] J. D. Morales, D. Blanco, D. P. Ruiz, and M. C. Carrion, "Non cooperative radar target identification using exponential single-mode extraction pulse," *IEEE Trans. Antennas Propag.*, vol. 59, no. 6, pp. 2445–2447, Jun. 2011.
[9] H.-S. Lui and N. V. Shuley, "Resonance based target recognition using ultrawideband polarimetric signatures," *IEEE Trans. Antennas Propag.*, vol. 60, no. 8, pp. 3985–3988, Aug. 2012.
[10] H. Zhang, Z. Fan, D. Ding, and R. Chen, "Radar target recognition based on multi-directional E-pulse technique," *IEEE Trans. Antennas Propag.*, vol. 61, no. 11, pp. 5838–5843, Nov. 2013.
[11] D. K. Singh, N. Mohan, D. C. Pande, and A. Bhattacharya, "A hybrid E-pulse method for discrimination of conducting scatterers in resonance region," *IEEE Trans. Antennas Propag.*, vol. 62, no. 8, pp. 4421–4425, Aug. 2014.
[12] Y. P. Zhou, Y. H. Chen, R. R. Gao, J. X. Feng, P. F. Zhao, and L. Wang, "SAR target recognition via joint sparse representation of monogenic components with 2D canonical correlation analysis," *IEEE Access*, vol. 7, pp. 25815–25826, 2019.
[13] R. Min, H. Lan, Z. Cao, and Z. Cui, "A gradually distilled CNN for SAR target recognition," *IEEE Access*, vol. 7, pp. 42190–42200, 2019.
[14] Z. He, H. Xiao, and Z. Tian, "Multi-view tensor sparse representation model for SAR target recognition," *IEEE Access*, vol. 7, pp. 48256–48264, 2019.
[15] B. Ding, G. Wen, X. Huang, C. Ma, and X. Yang, "Data augmentation by multilevel reconstruction using attributed scattering center for SAR target recognition," *IEEE Geosci. Remote Sens. Lett.*, vol. 14, no. 6, pp. 979–983, Jun. 2017.
[16] L. Du, L. Li, B. Wang, and J. Xiao, "Micro-Doppler feature extraction based on time-frequency spectrogram for ground moving targets classification with low-resolution radar," *IEEE Sensors J.*, vol. 16, no. 10, pp. 3756–3763, May 2016.
[17] M.-M. Zhao, Q. Zhang, Y. Luo, and L. Sun, "Micromotion feature extraction and distinguishing of space group targets," *IEEE Geosci. Remote Sens. Lett.*, vol. 14, no. 2, pp. 174–178, Feb. 2017.
[18] H. Gao, L. Xie, S. Wen, and Y. Kuang, "Micro-Doppler signature extraction from ballistic target with micro-motions," *IEEE Trans. Aerosp. Electron. Syst.*, vol. 46, no. 4, pp. 1969–1982, Oct. 2010.
[19] K. M. Li, X. J. Liang, Q. Zhang, Y. Luo, and H. J. Li, "Micromotion feature extraction and distinguishing of space group targets," *IEEE Geosci. Remote Sens. Lett.*, vol. 8, no. 3, pp. 411–415, May 2011.
[20] Y. Liu, S. Xing, Y. Li, D. Hou, and X. Wang, "Jamming recognition method based on the polarisation scattering characteristics of chaff clouds," *IET Radar, Sonar Navigat.*, vol. 11, no. 11, pp. 1689–1699, Nov. 2017.
[21] Y. Cheng, L. Gui, F. Hu, J. Su, B. Qi, S. Liu, and M. Huang, "Linear polarisation property and fusion method for target recognition in passive millimetre-wave polarimetric imaging," *Electron. Lett.*, vol. 52, no. 14, pp. 1221–1223, Jul. 2016.
[22] X. M. Jiang, Y. X. Lai, and M. Y. Xia, "Noise robust target identification based on the wave-coefficients-2dimension case," *Inverse Probl*, vol. 32, no. 12, pp. 1–13, 2016.
[23] X.-M. Jiang, S. Jia, M. Xia, and C. H. Chan, "Using wave-coefficients as feature vectors to identify aerospace targets," *Prog. Electromagn. Res.*, vol. 135, no. 1, pp. 465–480, 2013.
[24] M. J. Scolinik, *Introduction to Radar Systems*, 2nd ed. New York, NY, USA: McGraw-Hill, 1980.
[25] J. Wen, J. Weng, C. Tong, C. Ren, and Z. Zhou, "Sparse signal recovery with minimization of 1-Norm minus 2-Norm," *IEEE Trans. Veh. Technol.*, vol. 68, no. 7, pp. 6847–6854, Jul. 2019.
[26] J. Wen, L. Li, X. Tang, and W. H. Mow, "An efficient optimal algorithm for the successive minima problem," *IEEE Trans. Commun.*, vol. 67, no. 2, pp. 1424–1436, Feb. 2019.
[27] J. Wen, D. Li, and F. Zhu, "Stable recovery of sparse signals via lp-minimization," *Appl. Comput. Harmon. Anal.*, vol. 38, no. 1, pp. 161–176, Jan. 2015.
[28] W. J. Duncan, "LV. Applications of the Galerkin method to the torsion and flexure of cylinders and prisms," *London, Edinburgh, Dublin Phil. Mag. J. Sci.*, vol. 25, no. 169, pp. 634–649, Apr. 1938.

**XIAOMIN JIANG** received the B.Eng. degree in electronic information science and technology from Southwest Jiaotong University, Chengdu, China, in 2008, and the Ph.D. degree in electromagnetic fields and microwave technology from Peking University, Beijing, China, in 2013. He is currently a Lecturer with the Dongguan University of Technology. His main research interests are radar automatic target recognition (RATR), radar signal processing, and pattern recognition.

**YINGXIN LAI** (Member, IEEE) received the B.S. and Ph.D. degrees from Southwest Jiaotong University (SWJTU), Chengdu, China, in July 2003 and December 2008. He is currently an Associate Professor with the School of Electronic Engineering and Intelligentization, Dongguan University of Technology (DGUT), Dongguan, China. His research interests include microwave component design and radar signal processing.

**SHANJIN WANG** was born in Zhejiang, China, in 1966. He received the master's degree in physics from South China Normal University, Guangzhou, China, in 1992, and the Ph.D. degree in electrical engineering from Southeast University, Nanjing, China, in 2002. From 2002 to 2003, he was a Research Engineer with ZTE Corporation, Shenzhen, China. In June 2003, he joined the School of Electronic Engineering, Dongguan University of Technology, where he is currently a Professor. He has authored or coauthored a number of publications in the areas of microwave and antenna engineering. His current research interests include planar filters, planar antennas for wireless terminals, RF and microwave passive circuits, and inverse scattering problems.

**YUE SONG** was born in Baima, Shao Yang, Hunan, China, in 1963. He received the master's degree in signal and electric circuit and systematic specialty from Northwestern Polytechnical University, Xi'an, China, in 1991. Since 2003, he has been a Professor with the School of Electronic Engineering, Dongguan University of Technology. He is the author of two books, more than 100 articles, and more than 12 inventions. His research interests include electric circuit systems, measurement and control systems, and detection of radar target.